CrossMark
click for updates

View Article Online
View Journal

RSC Advances

This article can be cited before page numbers have been issued, to do this please use: J. Hua, J. Yang, H. Tan, D. Li, T. Jiang, Y. Gao, B. Li and X. Qu, *RSC Adv.*, 2016, DOI: 10.1039/C6RA11269B.

This is an *Accepted Manuscript*, which has been through the Royal Society of Chemistry peer review process and has been accepted for publication.

Accepted Manuscripts are published online shortly after acceptance, before technical editing, formatting and proof reading. Using this free service, authors can make their results available to the community, in citable form, before we publish the edited article. This *Accepted Manuscript* will be replaced by the edited, formatted and paginated article as soon as this is available.

You can find more information about *Accepted Manuscripts* in the Information for Authors.

Please note that technical editing may introduce minor changes to the text and/or graphics, which may alter content. The journal's standard Terms & Conditions and the Ethical guidelines still apply. In no event shall the Royal Society of Chemistry be held responsible for any errors or omissions in this *Accepted Manuscript* or any consequences arising from the use of any information it contains.

ROYAL SOCIETY OF CHEMISTRY

www.rsc.org/advances

View Article Online
DOI: 10.1039/C6RA11269B

Journal Name

RSCPublishing

ARTICLE

Published on 10 June 2016. Downloaded by California State University at Fresno on 12/06/2016 07:52:02.

Cite this: DOI: 10.1039/x0xx00000x

Synthesis, two-photon absorption and aggregation-induced emission properties of multi-branched triphenylamine derivatives based on diketopyrrolopyrrole for bioimaging

Received 00th January 2012,
Accepted 00th January 2012

DOI: 10.1039/x0xx00000x

www.rsc.org/

Ji Yang,[a] Haoqi Tan,[b] Dongyu Li,[c] Tao Jiang,[a] Yuting Gao,[a] Bo Li,[d] Xue Qu,*[b] Jianli Hua*[a]

In this work, three new diketopyrrolopyrrole (DPP)-based multi-branched derivatives **(YJ-1, YJ-2 and YJ-3)** with triphenylamine, 2,4,6-tri([1,1'-biphenyl]-4-yl)-1,3,5-triazine and 2,2',2''-(nitrilotr-is([1,1'-biphenyl]-4',4-diyl))tris(3-phenylacrylonitrile) cores have been designed and synthesized. Their one- and two-photon absorption properties have been investigated. The two-photon absorption cross sections (σ) measured by the open aperture Z-scan technique are determined to be 2912, 2016 and 2800 GM for **YJ-(1-3)**, respectively. This result indicates that donor–acceptor–donor (D–A–D)-type molecules are benefit to improve σ and their σ data increase with the better intramolec-ular charge transfer (ICT). Also, all of the three DPP derivatives exhibit good aggregation-induced emission (AIE) properties which are very weakly fluorescent in DMF, but a strong red fluorescent emission in solid state and in the aggregate state. More importantly, diketopyrrolopyrrole with tri-phenylamine **(YJ-1)** was applied for cell imaging and two-photon excited fluorescence in vivo imaging of mouse ear.

Introduction

The nonlinear optical (NLO) effect of two-photon absorption (2PA) has attracted widespread attention of the researchers in recent years. The extremely high intensity of a laser light beam allows an electronic excited state to be populated via the simultaneous absorption of two photons. 2PA has applications in many disparate fields such as 3D data storage and microfabrication, upconversion lasing, optical power limiting, photodynamic therapy, fluorescent probes, and bioimaging.[1-3] Due to the researchers' efforts, a series of new organic materials with large 2PA cross sections have been investigated. The molecular with extended π-conjugated systems functionalized by electron-donor (D) and/or electron-acceptor (A) groups designs including donor–acceptor–donor (D-A-D)-type, donor-π-bridge-acceptor (D-π-A)-type, donor–π-bridge–donor (D-π-D)-type macrocycles, and multi-branched molecules often show large 2PA cross sections (σ).[4] In addition, a combination of several pseudolinear subunits into a multidimensional structure is a familiar approach to assembling new chromophores, allowing variations in aspects such as the symmetry, length of the conjugated branches, and nature of the branching moiety.[5, 6]

To date, various fluorescent probes, including inorganic semiconductor quantum dots (QDs),[7] small organic dyes,[8] fluorescent proteins[9] have been exploited for two-photon fluorescence (2PF) bioimaging. However, these materials have some drawbacks, such as limited fluorescence stability of organic dyes and fluorescent proteins under long-term laser excitation,[10] potential toxicity and irregular blinking of QDs.[11] To improve the photo bleaching resistance, as well as brightness of organic dyes, one method is to increase their concentration. Whereas, most organic dyes suffer from a severe aggregation-caused quenching (ACQ) effect.[12] Recently, a novel phenomenon of aggregation-induced emission (AIE) is discovered that the AIE luminogens are nonemissive in good solvents and become highly emissive in aggregated state.[13-16] As far as we know, most studies on the AIE fluorophores for bioapplications are focused on the tetraphenylethylene (TPE) species with shorter wavelength input

[a] *Key Laboratory for Advanced Materials, Institute of Fine Chemicals and Department of Chemistry, East China University of Science and Technology, 130 Meilong Road, Shanghai, 200237, China. E-mail: jlhua@ecust.edu.cn; Fax:+86-21-64250940; Tel: +86-21-64250940*
[b] *The State Key Laboratory of Bioreactor Engineering and Key Laboratory for Ultrafine Materials of Ministry of Education. East China University of Science and Technology Shanghai. 200237, China.*
[c] *State Key Laboratory of Modern Optical Insrumentations and Center for Optical and Electromagnetic Research, Zhejiang University (ZJU), Hangzhou 310058, China.*
[d] *Key Laboratory of Polar Materials and Devices, Ministry of Education, East China Normal University, Shanghai 200241, China.*
† Electronic Supplementary Information (ESI) available: [details of any supplementary information available should be included here]. See http://www.rsc.org/suppdata/xx/b0/b000000x/

RSC Advances Accepted Manuscript

View Article Online
DOI: 10.1039/C6RA11269B
Journal Name

Published on 10 June 2016. Downloaded by California State University at Fresno on 12/06/2016 07:52:02.

and output signals.[17] The longer wavelength of the dyes have high tissue transparency and low autofluorescence in the long wavelength region.[18] Hence, it is still very essential to develop AIE materials with long wavelength emission and large 2PA cross sections for biological applications.

1,4-diketo-3,6-diphenylpyrrolo[3,4-c]pyrrole (DPP)-based high-performance materials have been well developed, such as OLEDs,[19] solar cells,[20] fluorescent probes[21-24] and two-photon absorption material[25] due to their excellent red and strongly fluorescent emission and brilliant light, weather, and heat stability, which could greatly expand the emission wavelength of dyes.[26] Previously, our group reported DPP-based red-emitting AIE materials with large σ which was used for cell imaging and two-photon blood vasculature imaging successfully.[27] Triarylamine is a traditional luminogen which has been widely used in opto- and electroactive materials for its good electron donating and transporting capability, as well as its special propeller starburst molecular structure.[28, 29] In addition, it would be a good unit for construction of multi-branched non-planar functional materials. Besides, 1,3,5-triazine-based compounds show good optical and electrical properties due to their high electron affinity and symmetrical structure. Recently, our group has presented multi-branched triphenylamine end-capped DPP derivatives incorporating an extended π-deficient phenylacrylonitrile that exhibited good 2PA and AIE properties.[27] To further understand their structure-properties correlation, we connect electron-donating triphenylamine to the 2,4,6-positions of triphenylamine, the triazine and the phenylacrylonitrile via DPP to form three new multibranched type 2PA derivatives with extended π-conjugated systems and good symmetry **(YJ-(1-3)**, **Scheme 1)**, respectively. Moreover, **YJ-1** was successfully used for one-photon laser scanning confocal microscopy cell imaging and two-photon vivo microscopic imaging of ear blood vessels of mice, indicating that compound **YJ-1** has great potential applicability in the bioapplications.

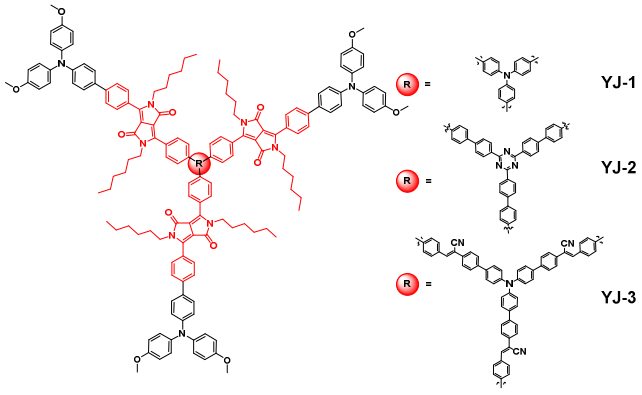

Scheme 1 Structures of **YJ-(1-3)** compounds.

Results and discussion

Synthesis

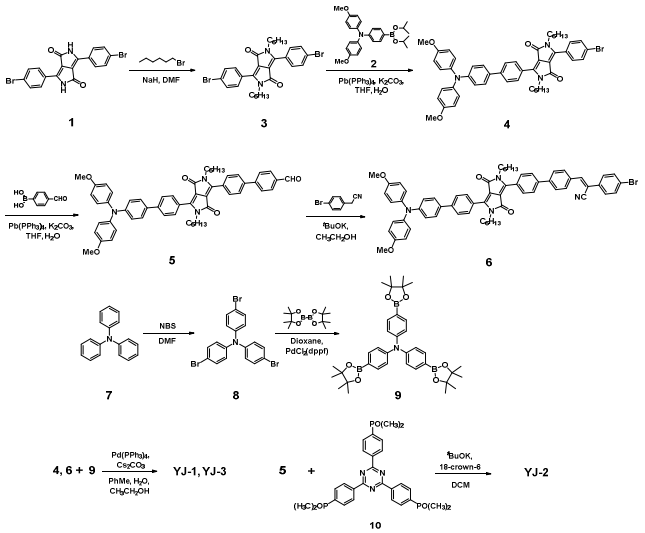

Scheme 2 Synthetic routes to **YJ-(1-3)** compounds

The synthetic routes of **YJ-(1-3)** are depicted in **Scheme 2**. The Suzuki coupling reaction of compound **2** with diisopropyl (4-(bis(4-methoxyphenyl)amino)phenyl) boronate **3** afforded compound **4**. The important intermediate aldehyde **5** was synthesized by a Suzuki coupling reaction of compound **4** and (4-formylphenyl)boronic acid. The tris(4-(4,4,5,5-tetramethyl-1,3,2-dioxaborolan-2-yl)phenyl)amine **9** with the respective DPP derivative (**4** and **6**) by the Suzuki reaction gave the target trilateral compounds **YJ-1** and **YJ-3**. The anoxicenvironment and potassium carbonate are the required parts of the Suzuki coupling. Finally, the target products **YJ-2** was synthesized by Horner-Wadsworth-Emmons reaction of the aldehydes (**5**) with 2,4,6-tri([1,1'-biphenyl]-4-yl)-1,3,5-triazine. The Horner-Wadsworth-Emmons reaction must use anhydrous reagents and be under no water environment. All compounds were purified by column chromatography or recrystallization and characterized by ^{1}H NMR, ^{13}C NMR and mass spectra (shown in ESI).

Photophysical properties

The **Fig. 1** shows the normalized one-photon absorption of **YJ-(1-3)** in DMF and in dispersion of the aggregate form (90% water) at 1×10^{-5} M. Their absorption maxima (λ_{max}) appeared at 519, 511 and 510 nm in dimethyl formamide (DMF), respectively. It is also noted that the absorption spectra of **YJ-(1-3)** in DMF/water (90% water in volume) mixtures are all broadened and red shifted by 10, 4 and 18 nm, respectively. The absorption tails extending well into the long wavelength region further indicated the aggregation of luminogen into particles in the presence of water, as it is well known that the Mie effect of particles causes such level-off tails in the absorption spectra.[30] Compared to **YJ-1**, the absorption maximum of **YJ-3** is blue shifted by 9 nm in DMF. The blue shifted may be caused by the introduction of the phenylacrylonitrile which block the ICT process. **YJ-2** is blue shifted by 8 nm compared to **YJ-1**, and it is possible that **YJ-2** has a more twisty structure, which hindered the intramolecular charge transfer.

RSC Advances Accepted Manuscript

This journal is © The Royal Society of Chemistry 2012

Journal Name
View Article Online
DOI: 10.1039/C6RA11269B
ARTICLE

Published on 10 June 2016. Downloaded by California State University at Fresno on 12/06/2016 07:52:02.

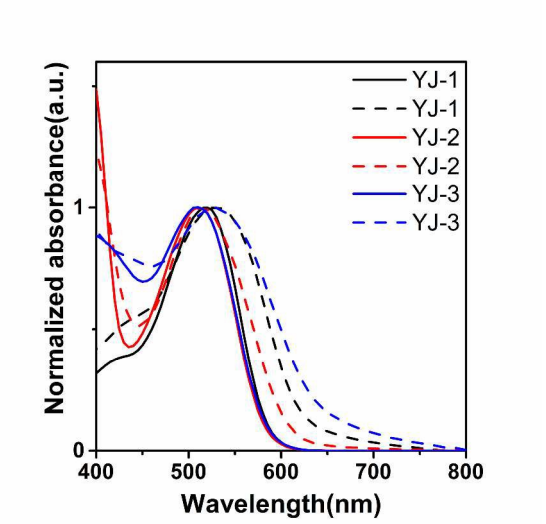

Fig. 1 Normalized one-photon absorption of **YJ-(1–3)** in DMF (solid line) and in dispersion of the nanoaggregate form (90% water) (dashed line) at 1×10^{-5} M

As expected, the dilute solution **YJ-1** in DMF had almost no fluorescence. But when the non-solvent water was gradually added into the solution in DMF, the solution started to emit fluorescence. After that, with the rising of water fraction in DMF, the fluorescence intensity of solution increased **(Fig. 2(A))**. When the water content reached to 50%, the fluorescence intensity of the solution was 19 times larger than that of the solution without water. The fluorescence peaks are nearly identical at 643 nm. This phenomenon is normal among the compounds with AIE properties, which could be caused by the variation in the packing mode of the molecules in aggregates.[30, 31] The aggregation of particles restricted the intramolecular rotation (RIR) process, which facilitated the radiative decay of the excitons, resulting in a strong increase in luminogen fluorescence. Similar behavior was observed for **YJ-2** and **YJ-3** in **Fig. 2(B and C)**, verifying that the three luminogens were AIE-active. The photo-luminescence intensity (PL) was very weak in the pure DMF, but when the water content reached to 80% and 70% in volume, **YJ-2** and **YJ-3** gave the maximum red luminescence and the peaks located at 651 nm and 672 nm with 40 and 32- increase, respectively. The fluorescence behavior of **YJ-(1-3)** is well visualized through fluorescence images of solution and aggregate dispersions as shown in **Fig. 2(E)**.

YJ-(1-3) are also investigated in the solid state, and their absolute fluorescence quantum yield (ϕ_F) were 7.30%, 8.32% and 6.08%, respectively **(Fig. (3A-3C))**. Moreover, to observe the formation of nanoparticles(NPs), the sizes distribution of **YJ-(1-3)** NPs were investigated by dynamic light scattering (DLS), indicating that the mean diameters are approximately 64 nm, 404 nm and 103 nm **(Fig. (3D-3F))**, respectively. Scanning electron microscopy (SEM) was also performed to study the morphology of the NPs, suggesting that they are in spherical shape with an average size of around 50 nm, 350 nm and 70 nm, respectively, which are slightly smaller than those of DLS due to the shrinking of samples in the vacuum dry state. All these given evidence

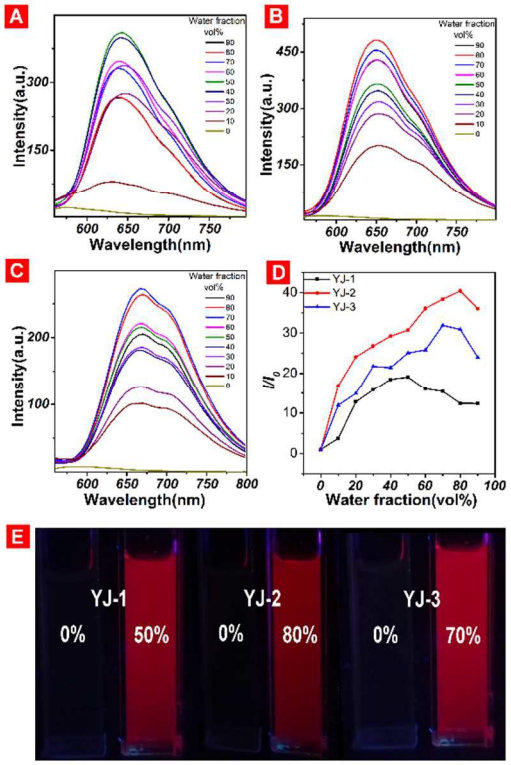

Fig. 2 (A, B and **C)** Corresponding emission spectra of compound **YJ- (1-3)** in DMF–water mixtures with different water fractions at 1×10^{-5} M. Excitation wavelength: 528 nm, 515nm, 532nm, respectively. **(D)** Plot of I/I_0 vs. water content of the solvent mixture, where I_0 is the PL intensity in pure DMF solution. **(E)** Photographs of **YJ-(1-3)** in the pure DMF solution and in 50%, 80%, 70% water-DMF mixture captured under UV light, respectively.

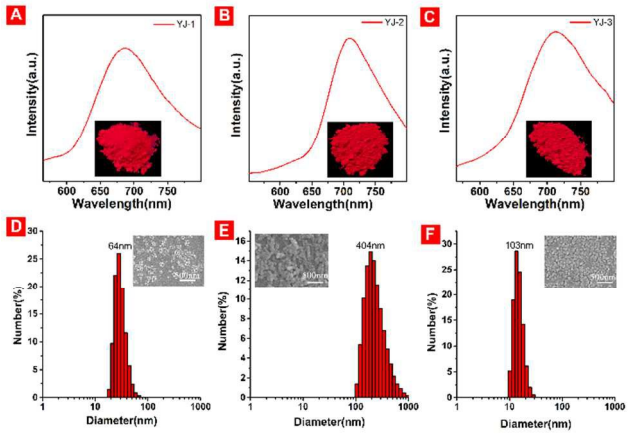

Fig. 3 Emission spectra of **YJ-(1-3) (A, B and C)** as solid powders; excitation wavelength: 519 nm for **YJ-1**, 511 nm for **YJ-2** and 510 nm for **YJ-3**. Inset: photos of **YJ-(1-3)** powders taken under illumination of a UV light (excitation wavelength: 365 nm). Particle size distribution and morphology of **(D) YJ-1** in DMF/H_2O (5: 5 v/v) and **(E) YJ-2** in DMF/H_2O (2: 8 v/v) **(F) YJ-3** in DMF/H_2O (3: 4 v/v) mixtures studied by DLS and SEM at the concentration of 1×10^{-5} M. The scale bar is 500 nm.

RSC Advances Accepted Manuscript

View Article Online
DOI: 10.1039/C6RA11269B
Journal Name

Published on 10 June 2016. Downloaded by California State University at Fresno on 12/06/2016 07:52:02.

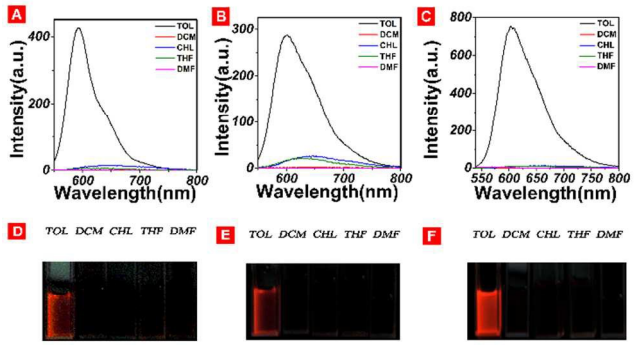

Fig. 4 (A, B and C) Emission spectra for **YJ-(1-3)** in different solvents at the concentration of 1×10^{-5}M. λ_{ex}: 528 nm **(YJ-1)** ,515 nm **(YJ-2)** and 532 nm **(YJ-3)**. **(D, E and F)** Photographs of **YJ-(1-3)** in different solvents under UV light.

indicated that the increasing PL intensity was caused by the increasing aggregation. Thus its AIE nature is adequately verified.

Meantime, we also investigated their optical properties in the different solvents, such as toluene (TOL), dichloromethane (DCM), chloroform(CHL), tetrahydrofuran (THF) and DMF. As shown in **Fig. S1-S3**, the absorption bands of the three compounds remain almost identical in the above solvents. However, a significant bathochromic shift of emission band and the decrease of fluorescence intensities can be observed with the increase in solvent polarity **(Fig. 4)**. Since the three dyes possess D-A structural units, such D-A molecules often show solvatochromic effects, which has been well explained by a twisted intramolecular charge transfer (TICT) mechanism.[32, 33] However, its emission intensity is weakened because of the susceptibility of the TICT state to various nonradiative quenching processes.

Two-photon absorption properties

2PA cross sections of **YJ-(1-3)** were determined by femtosecond open aperture Z-scan technique. **Fig. 5(1a-1c)** shows the open-aperture Z-scan data and 2PA coefficient obtained by data fitting. The σ can be calculated by using the equation of $\sigma = h\nu\beta N_0$, where $N_0 = N_A C$ is the number density of the absorption centers, N_A is the Avogadro constant and C represents the solute molar concentration and β is the 2PA coefficient.[34]The values of σ for **YJ-(1-3)** are 2912, 2016 and 2800 GM at wavelength of 800 nm, respectively. The values of **YJ-1** and **YJ-3** are larger than the **YJ-2**, because **YJ-1** and **YJ-3** have better π-systems. The smaller 2PA cross section of **YJ-3** (2800 GM) arises from the introduction of a phenylacrylonitrile in the π bridge compared to **YJ-1**, which may influence the molecular planarity. The two photon fluorescence spectrum of the three compounds under different laser intensities is shown in **Fig. 5(2a-2c)**. As shown in the inset, the linear dependence of fluorescence intensity on the square of the excitation intensity confirms that 2PA is the main

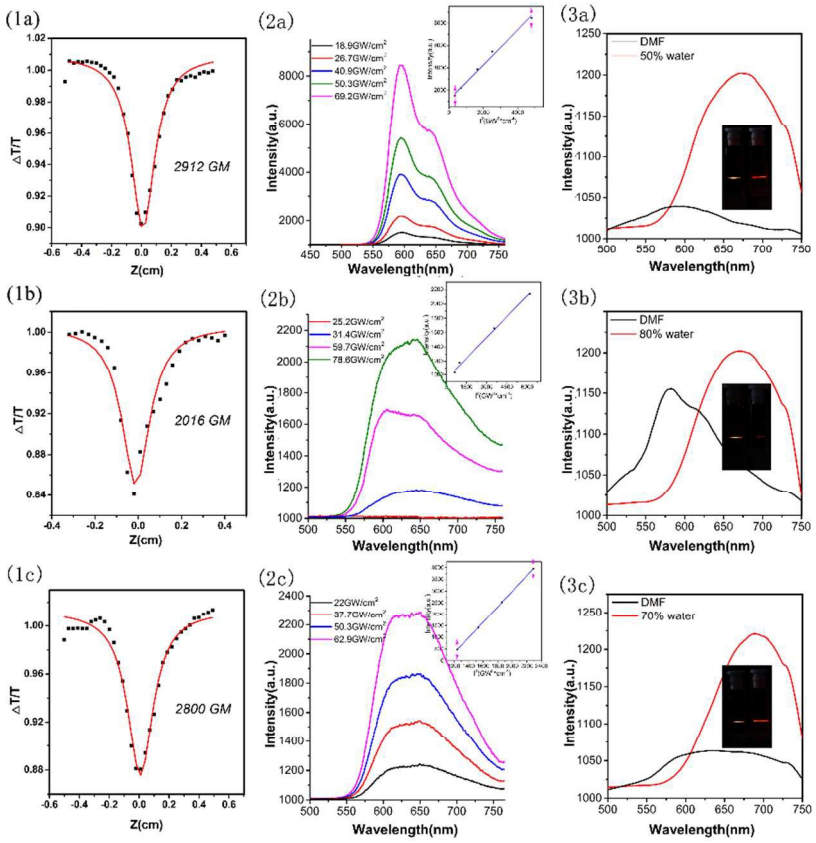

Fig. 5 (1a–1c) Open-aperture Z-scan trace of **YJ-(1–3)** (scattered circle experimental data, straight line theoretic fitted data). **(2a–2c)** 2PF intensities of **YJ-(1–3)** under different excitation power densities in toluene. **Inset:** 2PF intensity versus the square of the excitation power density. **(3a–3c)** Two-photon fluorescence emission spectra and 2PA emission images for **YJ-(1–3)** in DMF and in dispersion of the nanoaggregate form (50%, 80% and 70% water) at 1×10^{-5} M, excited at 800 nm. **YJ-1: 1a–3a; YJ-2: 1b–3b; YJ-3: 1c–3c.**

RSC Advances Accepted Manuscript

This journal is © The Royal Society of Chemistry 2012

View Article Online
DOI: 10.1039/C6RA11269B
ARTICLE

Published on 10 June 2016. Downloaded by California State University at Fresno on 12/06/2016 07:52:02.

excitation mechanism of the intense fluorescence emission.

Under the excitation of 80 fs pulse, 800 nm laser, **YJ-(1-3)** in the DMF/water mixtures emit NIR fluorescence with peaks located at 675 nm ,670 nm and 672 nm (**Fig. 5 (3a-3c)**), respectively. The two-photon excitation fluorescence is slightly red shifted compared with one-photon excitation due to reabsorption of partial emissive fluorescence. The overlap between one- and two-photon excitation fluorescence makes clear that the emissions resulted from the same excited state, regardless of the different modes of excitation. It shall be concentrated on that the studied three compounds have undergone two photon excitation studies at one wavelength (800 nm). As shown in the inset photos, the 2PF under the excitation of 800 nm laser was signally intensified by aggregation in DMF/water mixtures.

One-photon cellular imaging and two-photon luminescence vivo microscopic imaging of ear blood vessels of mice

Due to the good AIE and 2PA properties, high brightness in the near-infrared region, and the biggest two-photon absorption cross-section (σ) 2912 GM, the **YJ-1** was chosen as an example and their performance was investigated in one-photon cellular imaging and two-photon luminescence vivo microscopic imaging of ear blood vessels of mice. The cellular imaging in vitro was studied by confocal laser scanning microscopy (CLSM). In these experiments, MGC-803 cells are individually incubated in culture medium with **YJ-1** (1×10^{-6} M) for 4 h, and then imaged, as shown in **Fig. 6**. The nuclei are stained with 2-(4-amidinophenyl)-6-indolecarbamidine dihydrochloride (DAPI), which is a fluorescent dye that gives out blue emission, as shown in **Fig. 6(B)**. Red fluorescence is obviously observed in the cytoplasm of MGC-803 cells. The appearance of red fluorescence in the cytoplasm region of the cells surrounding the nucleus indicates that **YJ-1** is successfully endocytosed by cell lines and accumulated in the entire cell cytoplasm. In **Fig. 6(D)**, the fluorescence image is the overlaying images of **(A), (B)** and **(C)**. The cellular imaging of Hela cells with **YJ-1** was also investigated **(Fig. 6 (E-H))**. The size of **YJ-1** in DMSO/Dulbecco's modified Eagle's medium (DMEM) (1: 99 v/v) mixtures studied by DLS at concentration of 1×10^{-5}M indicated that the mean diameter is 89 nm while the mean diameters of DMEM studied by DLS is 28 nm **(Fig. S5-S6).** The mechanism of

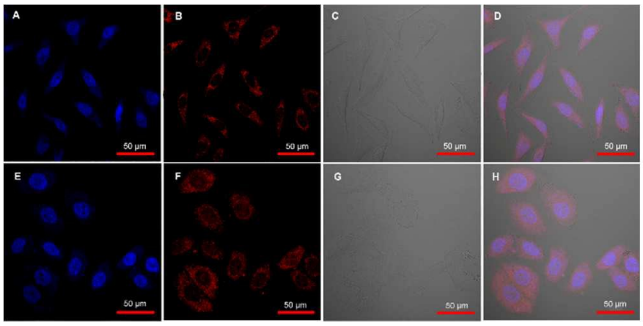

Fig. 6 MGC-803 cells **(A)** and HeLa cells of **(E)** fluorescence images of cells nuclei stained by DAPI; **(B) and (F)** fluorescence images of MGC-803 cells and Hela cells stained by **YJ-1**(1×10^{-6}M), respectively; **(C)** and **(G)** brightfield image of MGC-803 cells and Hela cells, respectively; **(D)** and **(H)** overlap image of **(A)**, **(B)**, **(C) and (E), (F), (G)**, respectively.

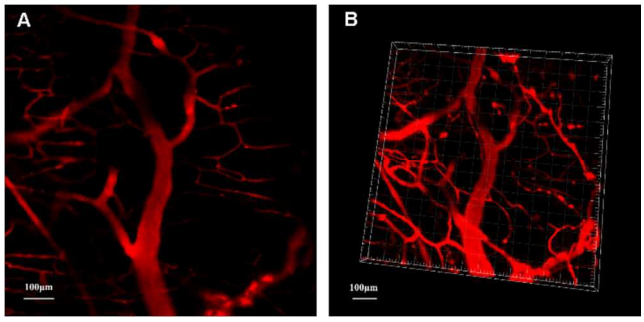

Fig. 7 Two-photon excited fluorescence **(A)** and reconstructed 3D image **(B)** the intravenously injected **YJ-1-PEG** nanoparticles in the blood vessel of the ear of a mouse.

cellular uptake of **YJ-1** might be the endocytosis process.[35-40] The metabolic viability of MGC-803 cells and Hela cells were further examined by methylthiazolyldiphenyltetrazolium bromide (MTT) assays, which revealed high cell viability of near 100% within 24 h even at a **YJ-1** concentration of 1×10^{-5} M, which is 10-fold higher than that used for imaging (**Fig. S4**).

To further investigate the ability of **YJ-1** for in-vivo two-photon fluorescence imaging, **YJ-1-PEG** nanoparticles[41] were synthesized to get stable micelle in order to improve the biocompatibility in blood vessels. Since samples were intravenously into mice, the blood vessels of mice were full of **YJ-1-PEG** due to blood circulation. Because of the bright 2PF signals from **YJ-1-PEG**, as well as low auto fluorescence of tissue under 800 nm fs excitation, the structure of blood vessels could be visualized clearly and the signal to noise ratio of the images was high even at 100μm deep of the mouse ear. As shown **(Fig. 7B)** the 3D reconstructed 2PF image of **YJ-1-PEG** in the mouse ear, the vascular architecture in the mouse ear was revealed clearly.

Conclusion

In this work, we have designed and synthesized three new multi-branched type and DPP-based chromophores **(YJ-(1-3))** with large 2PA cross sections and bright AIE fluorescence in water. Their σ values were 2912 GM, 2016 GM and 2800 GM, respectively. Investigation of the 2PA property of these compounds reveals that their 2PA cross section values increase with introducing multi-branched molecules and easier ICT progress around the molecules possible. Moreover, the **YJ-1** had the biggest two-photon absorption cross-section (σ) among the three dyes, so we choose the **YJ-1** as the fluorescence luminogen for bioimaging. Cellular imaging results indicated **YJ-1** could be utilized as a fluorescent probe for cellular imaging of 803 and HeLa cells, where red fluorescence was observed in the cytoplasm. In addition, 2PF in vivo imaging of mouse ear was conducted by using **YJ-1-PEG** as the contrast agents, and the 3D architecture of blood vessels was vividly reconstructed. The red emissive AIE nanoparticles with high 2PA efficiency at 800 nm would be useful for deep-tissue functional bioimaging in the future.

RSC Advances Accepted Manuscript

ARTICLE View Article Online
DOI: 10.1039/C6RA11269B Journal Name

Published on 10 June 2016. Downloaded by California State University at Fresno on 12/06/2016 07:52:02.

Experimental section

Materials and measurements

Tetrahydrofuran (THF) was pre-dried over 4 °A molecular sieves and distilled under argon atmosphere from sodium benzophenone ketyl immediately prior to use. N, N-Dimethyl formamide (DMF) and dichloromethane (DCM) were refluxed with calcium hydride and distilled before use. Compound **1**, compound **2**,[42] compound **9**[43]and compound **10**[17]were prepared according to previous literature protocols. All other reagents, proteins and fetal bovine serum were purchased from Sigma-Aldrich and used as received. The solutions for analytical studies were prepared with deionized water treated with a Milli-Q System (Billerica, MA, USA).

Instruments

^{1}H and ^{13}C NMR spectra were recorded on a Bruker AM-400 spectrometer using chloroform-d ($CDCl_3$) as solvent and tetramethylsilane (δ=0) as internal reference. The UV/vis spectra were recorded on a Varian-Cary 500 spectrophotometer with 2 nm resolution at room temperature. The fluorescence spectra were taken on a Varian-Cary fluorescence spectrophotometer. Time-resolved fluorescence measurements in this study were performed using the Edinburgh OB 900-L time-correlated single photon counting system (TCSPC). Emission was collected at right angle with respect to the pump. A temper deconvolution from the system response function, a temporal resolution of ~30 ps can be reliably obtained. The 2PA cross sections of **YJ-(1–3)** were measured by femtosecond open-aperture Z-scan technique according to a previously described method.[44] Two-photon excited fluorescence (2PF) was excited by fs pulses with different intensities at a wavelength of 800 nm. The repetition rate of the laser pulses was 250 kHz, and the pulse duration was 80 fs. The measurement was performed with a fixed scattering angle of 90°. The size of the nanoparticles was determined by an ALV-5000 laser light scattering spectrometer (DLS). The SEM micrographs were obtained on a JEOL JSM-6360 scanning electron microscope (SEM). The cell imaging experiments were carried out with an Olympus FV1000 laser scanning confocal microscope and a 60 × oil immersion objective lens.

Synthesis of 3,6-bis(4-bromophenyl)-2,5-dihexyl-2,5-dihydropyrrolo[3,4-c]pyrrole-1,4-dione (3)

To a suspension of **1** (500 mg, 1.1 mmol) in 10 mL N,*N*-Dimethylformamide (DMF) was added sodium hydride (108 mg, 4.4 mmol) with stirring at 0 °C. Then the mixture was warmed to room temperature (rt) and stirred for another 1.5 h. Then 1-bromohexane (0.64 mL, 4.4 mmol) was added dropwise. The mixture was stirred overnight at rt. After completion of the reaction, the mixture was poured into ice water, filtered, and then washed with water and hexane. The filter cake was dried under vacuum. The resulting crude product was purified by column chromatography on silica gel (eluent: DCM/petroleum ether (1: 1, v/v) to obtain **3** (310 mg, 45.01% yield) as an orange-red solid.

Synthesis of 3-(4'-(bis(4-methoxyphenyl)amino)-[1,1'-biphen-yl]-4-yl)-6-(4-brom-ophenyl)-2,5-dihexyl-2,5-dihydropyrrolo-[3,4-c]pyrrole-1,4-dione (4)

A mixture of **3** (738 mg, 1.2 mmol), **2** (434 mg, 1.0 mmol), and $Pd(PPh_3)_4$ (21 mg, 0.02 mmol) was dissolved in 15 mL THF under argon atmosphere. Aqueous potassium carbonate solution (2 M, 5 mL) was added to the reaction solution and stirred at 40 °C for 3 h. After cooling to room temperature, the reaction mixture was extracted by di-chloromethane (3 × 15 mL). The combined organic layer was washed with water and dried over Na2SO4. After removal of the solvent, the crude product was purified by column chromatography on silica gel (eluent: DCM/petroleum ether (3:1, v/v) to obtain **4** (270 mg, 32% yield) as a red solid. ^{1}H NMR (400 MHz, Chloroform-*d*) δ 7.89 (d, *J* = 8.2 Hz, 2H), 7.74-7.64 (m, 6H), 7.47 (d, *J* = 8.8 Hz, 2H), 7.14-7.09 (m, 4H), 6.99 (d, *J* = 8.2 Hz, 2H), 6.89-6.84 (m, 4H), 3.83-3.80 (m, 6H), 3.79-3.68 (m, 4H), 1.28-1.21 (m, 12H), 0.94-0.74 (m, 10H); ^{13}C NMR (101 MHz, Chloroform-*d*) δ 162.64, 156.19, 149.01, 146.37, 143.58, 140.48, 132.14, 131.06, 130.14, 129.28, 127.59, 126.97, 126.46, 120.10, 114.80, 109.39, 55.50, 31.24, 29.41, 26.42, 22.50, 14.00; MALDI-TOF: [M^+] calcd for $C_{50}H_{52}BrN_3O_4$: 837.3141, found: 837.3142.

Synthesis of 4'-(4-(4'-(bis(4-methoxyphenyl)amino)-[1,1'-biphenyl]-4-yl)-2,5-di-hexyl-3,6-dioxo-2,3,5,6-tetrahydropyrrolo-[3,4-c]pyrrol-1-yl)-[1,1'-biphenyl]-4-carba-ldehyde (5)

A mixture of **4** (839 mg, 1.0 mmol), (4-formylphenyl)boronic acid (300 mg, 2.0 mmol), and $Pd(PPh_3)_4$ (21 mg, 0.02 mmol) was dissolved in 15 mL THF under argon atmosphere. Aqueous potassium carbonate solution (2 M, 5 mL) was added to the reaction solution and stirred at 60 °C for 12 h. After cooling to room temperature, the reaction mixture was extracted by DCM (3 × 15 mL). The combined organic layer was washed with water and dried over Na2SO4. After removal of the solvent, the crude product was purified by column chromatography on silica gel (eluent: DCM/petroleum ether (5:1, v/v) to obtain **5** (650 mg, 75% yield) as a red solid. ^{1}H NMR (400 MHz, Chloroform-*d*) δ: 10.02 (s, 1H), 7.91 (dd, *J* = 16.7, 8.1 Hz, 4H), 7.83 (d, *J* = 8.3 Hz, 2H), 7.78-7.71 (m, 4H), 7.64 (d, *J* = 8.2 Hz, 2H), 7.43-7.38 (m, 2H), 7.05 (d, *J* = 8.8 Hz, 4H), 6.92 (d, *J* = 8.8 Hz, 2H), 6.80 (d, *J* = 8.8 Hz, 4H), 3.81-3.69 (m, 10H), 1.54-1.52 (m, 4H), 1.19 (t, *J* = 9.7 Hz, 16H), 0.76 (t, *J* = 6.4 Hz, 6H); ^{13}C NMR (101 MHz, Chloroform-*d*) δ: 191.81, 162.79, 156.20, 148.94, 146.96, 145.83, 143.59, 141.93, 140.45, 135.66, 131.03, 130.40, 129.39, 129.30, 128.34, 127.73, 127.57, 127.00, 126.48, 125.89, 120.03, 114.80, 110.31, 109.55, 67.99, 55.50, 31.26, 26.45, 25.63, 22.51, 14.01; HRMS (ESI) (m/z): [M^+] calcd for $C_{57}H_{57}N_3O_5$: 863.4298, found: 863.4296.

Synthesis of 3-(4'-(4-(4'-(bis(4-methoxyphenyl)amino)-[1,1'-biphenyl]-4-yl)-2,5-dihexyl-3,6-dioxo-2,3,5,6-tetrahydropyrrolo[3,4-c]pyrrol-1-yl)-[1,1'-biphenyl]-4-yl)-2-(4-bromophenyl)acrylonitrile (6)

A mixture of **5** (864 mg, 1.0 mmol), 2-(4-bromophenyl)acetonitrile (392 mg, 2.0 mmol), and Potassium tert-butylate (KTB) (448 mg, 4.0 mmol) was dissolved in 20 mL ethanol under argon atmosphere. The mixture was stirred at 50 °C for 12 h. After cooling to room temperature, the reaction mixture was removed under vacuum. Then the mixture was extracted by DCM (10 mL) and water (3 × 5 mL). The combined organic layer was washed with water and dried over Na_2SO_4.

RSC Advances Accepted Manuscript

This journal is © The Royal Society of Chemistry 2012

View Article Online
DOI: 10.1039/C6RA11269B ARTICLE

Published on 10 June 2016. Downloaded by California State University at Fresno on 12/06/2016 07:52:02.

After removal of the solvent, the crude product was purified by column chromatography on silica gel (eluent: DCM/petroleum ether (15:1, v/v) to obtain **6** (860 mg, 83% yield) as a red solid. ^{1}H NMR (400 MHz, Chloroform-*d*) δ: 7.93 (d, *J* = 8.1 Hz, 2H), 7.87 (d, *J* = 8.2 Hz, 2H), 7.83 (d, *J* = 8.1 Hz, 2H), 7.71 (dd, *J* = 14.0, 8.1 Hz, 4H), 7.62 (d, *J* = 7.9 Hz, 2H), 7.55-7.37 (m, 8H), 7.19 (s, 1H), 7.03 (d, *J* = 10.9 Hz, 4H), 6.80 (d, *J* = 8.0 Hz, 4H), 3.89-3.62 (m, 10H), 1.20-1.15 (m, 16H), 0.80-0.74 (m, 6H); ^{13}C NMR (101 MHz, Chloroform-*d*) δ: 162.81, 156.17, 148.94, 148.72, 147.19, 143.51, 142.07, 141.73, 140.48, 133.18, 132.27, 131.09, 130.05, 129.39, 129.30, 127.89, 127.57, 127.46, 127.36, 126.97, 126.47, 125.93, 123.55, 120.09, 117.73, 114.80, 110.54, 110.17, 109.57, 55.52, 42.07, 31.27, 29.73, 26.47, 22.52, 14.02; HRMS (ESI) (m/z): [M^+] calcd for $C_{65}H_{61}BrN_4O_4$: 1040.3876, found: 1040.3895.

Synthesis of tris(4-bromophenyl)amine (8)

To a double-neck round bottom flask (250 mL) which equipped with mechanical stirrer were charged triphenylamine (3 g, 12.23 mmol) and DMF (100 mL). A DMF (20 mL) solution of N-bromosuccinimide (9.79 g, 55.03 mmol) was dropwisely added to the reaction flask. After addition of the DMF solution, the mixture was kept stirring for 1 h. The reaction was quenched with water and extracted with ethyl acetate (100 mL × 3). The organic layer was washed by NH_4Cl solution, then separated and dried over anhydrous MgSO4. The solution was filtered and evaporated to remove the solvent. The crude product was purified by column chromatography on silica gel (eluent: petroleum) to obtain **8** (5.1 g, 87%yield) as a white solid. ^{1}H NMR (400 MHz, Chloroform-*d*) δ: 7.38 (d, *J* = 8.4 Hz, 6H), 6.95 (d, *J* = 8.5 Hz, 6H).

Synthesis of 4,4',4''-Tris(pinacolatoborane)phenylamine) (9)

A mixture of **8** (1.93 g, 4.0 mmol), bis(pinacolato)diboron (3.75 g, 3.69 mmol), [1,1'-Bis(diphenyl-phosphino)ferrocene]-palladium(II) chloride (147 mg, 0.2 mmol)and potassium acetate (7 g, 71.33 mmol) was dissolved in 55 mL dioxane under argon atmosphere. The mixture was stirred at 85 °C for 12 h. After cooling to room temperature, the reaction mixture was removed under vacuum. Then the mixture was extracted by dichlo-romethane (30 mL) and water (3 × 15 mL). The combined organic layer was washed with water and dried over Na_2SO_4. After removal of the solvent, the crude product was purified by column chromatography on silica gel (eluent: DCM/petroleum ether (1:2, v/v) to obtain **9** (500 mg, 20% yield) as a white solid. ^{1}H NMR (400 MHz, Chloroform-*d*) δ: 7.68 (d, *J* = 8.1 Hz, 6H), 7.07 (d, *J* = 8.0 Hz, 6H), 1.34 (s, 36H).

Synthesis of 6,6',6''-(nitrilotris([1,1'-biphenyl]-4',4-diyl))tris-(3-(4'-(bis(4-metho-xyphenyl)amino)-[1,1'-biphenyl]-4-yl)-2,5-dihexyl-2,5-dihydropyrrolo[3,4-c]pyrrole-1,4-dione) (YJ-1)

A mixture of **4** (470 mg, 0.56 mmol), **9** (89 mg, 0.14 mmol), and $Pd(PPh_3)_4$ (5 mg, 0.001 mmol) was dissolved in methylbenzene (21 mL) and ethanol (7mL) under argon atmosphere. Aqueous potassium carbonate solution (2 M, 5 mL) was added to the reaction solution and stirred at 105 °C for 72 h. After cooling to room temperature, the reaction mixture was extracted by DCM (3 × 15 mL). The combined organic layer was washed with water and dried over Na2SO4. After removal of the solvent, the crude product was purified by column chromatography on silica gel (eluent: DCM/petroleum ether (15:1, v/v) to obtain **YJ-1** (200 mg, 55% yield) as a red solid. ^{1}H NMR (400 MHz, Chloroform-*d*) δ: 7.80 (d, *J* = 8.1 Hz, 6H), 7.73 (d, *J* = 8.0 Hz, 6H), 7.59 (d, *J* = 8.1 Hz, 6H), 7.48 (dd, *J* = 15.1, 8.2 Hz, 12H), 7.32 (d, *J* = 8.3 Hz, 6H), 7.22-7.15 (m, 6H), 7.01 (d, *J* = 8.5 Hz, 12H), 6.92-6.84 (m, 6H), 6.77 (d, *J* = 8.9 Hz, 12H), 3.73 (s, 30H), 1.17 (q, *J* = 10.6, 8.6 Hz, 48H), 0.75 (q, *J* = 6.9, 5.4 Hz, 18H); ^{13}C NMR (101 MHz, Chloroform-*d*) δ: 161.69, 155.05, 150.48, 147.70, 147.32, 146.73, 145.94, 139.47, 134.72, 133.42, 130.16, 128.43, 128.27, 126.98, 126.49, 125.87, 125.56, 125.17, 124.49, 123.48, 119.07, 113.74, 108.63, 108.42, 54.43, 33.19, 30.22, 29.28, 25.41, 21.46, 12.95; MALDI-TOF: [M^+] calcd for $C_{168}H_{168}N_{10}O_{12}$: 2517.2843, found: 2517.2878.

Synthesis of 6,6',6''-((((1,3,5-triazine-2,4,6-triyl)tris(benzene-4,1-diyl))tris(e-thene-2,1-diyl))tris([1,1'-biphenyl]-4',4-diyl))-tris(3-(4'-(bis(4-methoxyphenyl)amino)-[1,1'-biphenyl]-4-yl)-2,5-dihexyl-2,5-dihydropyrrolo[3,4-c]pyrrole-1,4-dione)(YJ-2)

In a 100 mL round-bottom flask, **5** (361 mg, 0.42 mmol), **10** (71 mg, 0.1 mmol), potassium tert-butoxide (117 mg, 1.05 mmol), 18-crown-6 (10 mg, 0.04 mmol) and 50 mL DCM were added under argon atmosphere. After stirring at 45 °C for 6 h, the mixture was poured into distilled water and extracted with DCM and water. The combined organic phases were dried over anhydrous MgSO4 and concentrated using a rotary evaporator. The crude product was purified by column chromatography on silica gel (eluent: DCM/petroleum ether (20:1, v/v) to obtain **YJ-2** (185 mg, 61% yield) as a red solid. ^{1}H NMR (400 MHz, Chloroform-*d*) δ: 8.31 (d, *J* = 7.7 Hz, 6H), 7.63 (d, *J* = 7.7 Hz, 6H), 7.54 (d, *J* = 7.8 Hz, 6H), 7.41-7.22 (m, 30H), 7.21-7.14 (m, 6H), 7.00-6.88 (m, 18H), 6.80 (d, *J* = 8.2 Hz, 6H), 6.73 (d, *J* = 8.6 Hz, 12H), 3.71 (s, 30H), 1.20-1.06 (m, 48H), 0.73 (t, *J* = 6.6 Hz, 18H); ^{13}C NMR (101 MHz, Chloroform-*d*) δ: 169.17, 161.41, 161.30, 154.95, 150.49, 147.49, 147.38, 146.54, 141.43, 140.84, 139.49, 134.73, 130.16, 128.42, 127.22, 126.42, 125.82, 125.19, 124.69, 124.50, 119.07, 113.73, 108.34, 108.01, 54.41, 33.20, 30.21, 29.29, 25.42, 21.48, 12.96; MALDI-TOF: [M^+] calcd for $C_{195}H_{186}N_{12}O_{12}$: 2887.4313, found: 2887.4312.

Synthesis of 2,2',2''-(nitrilotris([1,1'-biphenyl]-4',4-diyl))-tris(3-(4'-(4-(4'-(bis(4-methoxyphenyl)amino)-[1,1'-biphenyl]-4-yl)-2,5-dihexyl-3,6-dioxo-2,3,5,6-tetrahydropyrrolo-[3,4-c]-pyrrol-1-yl)-[1,1'-biphenyl]-4-yl)acrylonitrile) (YJ-3)

A mixture of **6** (261 mg, 0.25 mmol), **9** (39 mg, 0.06 mmol), and $Pd(PPh_3)_4$ (5 mg, 0.001 mmol) was dissolved in methylbenzene (21 mL) and ethanol (7 mL) under argon atmosphere. Aqueous potassium carbonate solution (2 M, 5 mL) was added to the reaction solution and stirred at 105 °C for 72 h. After cooling to room temperature, the reaction mixture was extracted by DCM (3 × 15 mL). The combined organic layer was washed with water and dried over Na2SO4. After removal of the solvent, the crude product was purified by column chromatography on silica gel (eluent: DCM/petroleum ether (20:1, v/v) to obtain **YJ-3** (115 mg, 59% yield) as a red solid. ^{1}H NMR (400 MHz, Chloroform-*d*) δ: 7.91 (d, *J* = 7.9 Hz, 6H), 7.83 (d, *J* = 8.0 Hz, 6H), 7.72 (dd,

RSC Advances Accepted Manuscript

View Article Online
DOI: 10.1039/C6RA11269B Journal Name

Published on 10 June 2016. Downloaded by California State University at Fresno on 12/06/2016 07:52:02.

J = 22.2, 8.1 Hz, 18H), 7.65-7.55 (m, 18H), 7.54-7.45 (m, 12H), 7.36 (d, *J* = 8.6 Hz, 6H), 7.22 (d, *J* = 8.6 Hz, 6H), 7.10 (dd, *J* = 18.0, 8.8 Hz, 12H), 6.94 (d, *J* = 8.4 Hz, 3H), 6.85 (t, *J* = 10.3 Hz, 12H), 3.81 (d, *J* = 3.6 Hz, 30H), 1.23 (d, *J* = 22.0 Hz, 48H), 0.81 (d, *J* = 6.9 Hz, 18H); ^{13}C NMR (101 MHz, Chloroform-*d*) δ: 161.55, 155.02, 147.76, 146.19, 139.49, 130.13, 128.88, 128.49, 128.36, 126.83, 126.46, 126.07, 125.86, 125.25, 124.87, 123.43, 119.06, 113.75, 108.70, 108.13, 54.44, 30.20, 28.68, 28.10, 25.40, 21.46, 12.94; MALDI-TOF: [M^+] calcd for $C_{213}H_{195}N_{13}O_{12}$: 3128.5115, found: 3128.5300.

Cell Culture

All cells were purchased from the American Type Culture Collection (ATCC). cells were grown in DMEM supplemented with 10% fetal bovine serum (FBS) and 100 U/mL penicillin and 100 μg/mL streptomycin and cultured in 75 cm^2 tissue culture flasks in a humidified 5% CO_2 environmental incubator at 37 °C and cultivated at 80% confluency.
The cultured cells were harvested with 0.05/0.02% trypsin /EDTA, centrifuged at 800 rpm for 4 min and resuspended in the culture medium, followed by cell-counting using a haemocytometer.

Cytotoxicity Assay by MTT

MGC-803 and Hela Cells were seeded in 96-well plates with a confluence of about 8000 cells/well. After incubation for 24 h at 37 °C, 200 μL fresh culture medium containing **YJ-1** nanoparticles with the concentrations 10 μM, was added into the different cell plates. After another 24 h incubation, 30 μL MTT solution (5 mg/mL) were added to each well and the plates were incubated for another 4 h at 37 °C. Than the medium was removed and the yielded purple formazan crystals inside cells were dissolved by DMSO and OD values were measured at 492 nm using a a microplate reader (SPECTRAmax 384, Molecular Devices, USA) .

Cell imaging by CLSM:

In these experiments, cells were fixed with 2.5% glutaraldehyde solution for 15 min after 4 h incubation of cells in culture medium with **YJ-1** (10^{-6}M). Then, the fixed cells were attained with 5 μg/mL of DAPI for 15 min for nuclei staining. Cell images were observed using confocal laser scaning microscopy (CLSM, Nikon, Japan).

Synthesis of YJ-1-PEG nanoparticles

500 μL of **YJ-1** in chloroform solution (2 mg/mL) was added to 400 μL of DSPE-$mPEG_{5000}$ in chloroform solution (10 mg/mL). After sonicated for several minutes, the mixture was dried under vacuum in a rotary evaporator at 35 °C to remove the chloroform. 500 μL of DI water was then added into the flask and the solution was sonicated. Finally, suspension containing **YJ-1-PEG** nanoparticles was prepared.

Animals

Female white mice (ICR line) were obtained from the Laboratory Animal Center of Zhejiang University (Hangzhou, China). Mice were housed in cages in groups (5 mice per cage) and fed with standard mouse chow and water. The cages were maintained in a room with controlled temperature (25 61 uC) and a 12 h light/dark cycle. The protocol of animal experiments was approved by the Institutional Ethical Committee of Animal Experimentation of Zhejiang University in China, and the experiments were performed strictly according to governmental and international guidelines on animal experimentation. According to requirements for Biosafety and Animal Ethics, all efforts were made to minimize the number of animals used and their suffering.

Acknowledgements

For financial support of this research, we thank the National Basic Research 973 Program (2013CB733700), and NSFC/China (21421004, 21172073, 21372082, 21572062, 91233207 and 51573047).

Notes and references

1. G. S. He, L. S. Tan, Q. Zheng and P. N. Prasad, *Chem. Rev.*, 2008, **108**, 1245-1330.
2. M. Pawlicki, H. A. Collins, R. G. Denning and H. L. Anderson, *Angew. Chem.*, 2009, **48**, 3244-3266.
3. H. Myung Kim and B. Rae Cho, *Chem. Commun.*, 2009, **2**, 153-164.
4. Y. Jiang, Y. Wang, B. Wang, J. Yang, N. He, S. Qian and J. Hua, *Chem. Asian J.*, 2011, **6**, 157-165.
5. Y. Jiang, Y. Wang, J. Hua, J. Tang, B. Li, S. Qian and H. Tian, *Chem. Commun.*, 2010, **46**, 4689-4691.
6. G. S. He, J. Swiatkiewicz, Y. Jiang, P. N. Prasad, B. A. Reinhardt, L. S. Tan and R. Kannan, *J. Phys. Chem. A*, 2000, **104**, 4805-4810.
7. D. R. Larson, W. R. Zipfel, R. M. Williams, S. W. Clark, M. P. Bruchez, F. W. Wise and W. W. Webb, *Science*, 2003, **300**, 1434-1436.
8. M. J. Miller, S. H. Wei, I. Parker and M. D. Cahalan, *Science*, 2002, **296**, 1869-1873.
9. M. Drobizhev, N. S. Makarov, S. E. Tillo, T. E. Hughes and A. Rebane, *Nature Methods*, 2011, **8**, 393-399.
10. H. Wang, T. B. Huff, D. A. Zweifel, W. He, P. S. Low, A. Wei and J. X. Cheng, *Proc. Natl. Acad. Sci. U. S. A.*, 2005, **102**, 15752-15756.
11. E. Betzig, G. H. Patterson, R. Sougrat, O. W. Lindwasser, S. Olenych, J. S. Bonifacino, M. W. Davidson, J. Lippincott-Schwartz and H. F. Hess, *Science*, 2006, **313**, 1642-1645.
12. R. Ullah and J. Dutta, *J. Hazard, Mater,*, 2008, **156**, 194-200.
13. X. Zhang, X. Zhang, L. Tao, Z. Chi, J. Xu and Y. Wei, *J. Mater. Chem. B*, 2014, **2**, 4398-4414.
14. Y. Wang, R. Hu, W. Xi, F. Cai, S. Wang, Z. Zhu, R. Bai and J. Qian, *Biomed. Opt. Express*, 2015, **6**, 3783-3794.
15. K. Li and B. Liu, *Chem. Soc. Rev.*, 2014, **43**, 6570-6597.
16. T. Jiang, Y. Qu, B. Li, Y. Gao and J. Hua, *RSC Adv.*, 2015, **5**, 1500-1506.
17. Y. Gao, Y. Qu, T. Jiang, H. Zhang, N. He, B. Li, J. Wu and J. Hua, *J. Mater. Chem. C*, 2014, **2**, 6353-6361.
18. T. Myochin, K. Hanaoka, S. Iwaki, T. Ueno, T. Komatsu, T. Terai, T. Nagano and Y. Urano, *J. Am. Chem. Soc.*, 2015, **137**, 4759-4765.

RSC Advances Accepted Manuscript

This journal is © The Royal Society of Chemistry 2012

View Article Online
DOI: 10.1039/C6RA11269B ARTICLE

Published on 10 June 2016. Downloaded by California State University at Fresno on 12/06/2016 07:52:02.

19. Y. Zhu, A. R. Rabindranath, T. Beyerlein and B. Tieke, *Macromolecules*, 2007, **40**, 6981-6989.
20. F. Liu, C. Wang, J. K. Baral, L. Zhang, J. J. Watkins, A. L. Briseno and T. P. Russell, *J. Am. Chem. Soc.*, 2013, **135**, 19248-19259.
21. X. Zhang, Y. Hang, W. Qu, Y. Yan, P. Zhao and J. Hua, *RSC Adv.*, 2016, **6**, 20014-20020.
22. W. Qu, L. Yang, Y. Hang, X. Zhang, Y. Qu and J. Hua, *Sens. Actuators B*, 2015, **211**, 275-282.
23. Y. Hang, L. Yang, Y. Qu and J. Hua, *Tetrahedron Letters*, 2014, **55**, 6998-7001.
24. Y. Hang, J. Wang, T. Jiang, N. Lu and J. Hua, *Anal. Chem.*, 2016, **88**, 1696-1703.
25. E. Q. Guo, P. H. Ren, Y. L. Zhang, H. C. Zhang and W. J. Yang, *Chem. Commun.*, 2009, **39**, 5859-5861.
26. H. Patil, A. Gupta, A. Bilic, S. V. Bhosale and S. V. Bhosale, *Tetrahedron Letters*, 2014, **55**, 4430-4432.
27. Y. Gao, G. Feng, T. Jiang, C. Goh, L. Ng, B. Liu, B. Li, L. Yang, J. Hua and H. Tian, *Adv. Funct. Mater.*, 2015, **25**, 2857-2866.
28. Z. Ning and H. Tian, *Chem. Commun.*, 2009, **37**, 5483-5495.
29. G. Tu, S. Massip, P. M. Oberhumer, X. He, R. H. Friend, N. C. Greenham and W. T. S. Huck, *J. Mater. Chem.*, 2010, **20**, 9231-9238.
30. B. Z. Tang, Y. Geng, J. W. Y. Lam, B. Li, X. Jing, X. Wang, F. Wang, A. B. Pakhomov and X. X. Zhang, *Chem. Mater.*, 1999, **11**, 1581-1589.
31. Y. Ren, Y. Dong, J. W. Y. Lam, B. Z. Tang and K. S. Wong, *Chem. Phys. Lett.*, 2005, **402**, 468-473.
32. W. Qin, D. Ding, J. Liu, W. Z. Yuan, Y. Hu, B. Liu and B. Z. Tang, *Adv. Funct. Mater.*, 2012, **22**, 771-779.
33. X. Y. Shen, W. Z. Yuan, Y. Liu, Q. Zhao, P. Lu, Y. Ma, I. D. Williams, A. Qin, J. Z. Sun and B. Z. Tang, *J. Phys. Chem. C*, 2012, **116**, 10541-10547.
34. Y. Gao, H. Zhang, T. Jiang, J. Yang, B. Li, Z. Li and J. Hua, *Science China Chemistry*, 2013, **56**, 1204-1212.
35. M. Li, C. Y. Nie, L. H. Feng, H. X. Yuan, L. B. Liu, F. T. Lv and S. Wang, *Chem-Asian J*, 2014, **9**, 3121-3124.
36. M. Li, Y. N. Hong, Z. K. Wang, S. J. Chen, M. Gao, R. T. K. Kwok, W. Qin, J. W. Y. Lam, Q. C. Zheng and B. Z. Tang, *Macromol. Rapid Commun.*, 2013, **34**, 767-771.
37. Y. Bao, H. De Keersmaecker, S. Corneillie, F. Yu, H. Mizuno, G. Zhang, J. Hofkens, B. Mendrek, A. Kowalczuk and M. Smet, *Chem. Mater.*, 2015, **27**, 3450-3455.
38. Z. Zhou, C. C. Zhang, Y. Zheng and Q. Wang, *J. Med. Chem.*, 2016, **59**, 410-418.
39. A. Kurtz-Chalot, J. P. Klein, J. Pourchez, D. Boudard, V. Bin, O. Sabido, L. Marmuse, M. Cottier and V. Forest, Biomed. Microdevices, 2015, **17**, 1-12.
40. C. W. Evans, M. Fitzgerald, T. D. Clemons, M. J. House, B. S. Padman, J. A. Shaw, M. Saunders, A. R. Harvey, B. Zdyrko, I. Luzinov, G. A. Silva, S. A. Dunlop and K. S. Iyer, Acs Nano, 2011, **5**, 8640-8648.
41. D. Wang, J. Qian, S. He, J. S. Park, K. S. Lee, S. Han and Y. Mu, *Biomaterials*, 2011, **32**, 5880-5888.
42. Y. Hang, X. P. He, L. Yang and J. Hua, *Biosens. Bioelectron.*, 2014, **65C**, 420-426.
43. G. Wang, K.-Y. Pu, X. Zhang, K. Li, L. Wang, L. Cai, D. Ding, Y.-H. Lai and B. Liu, *Chem. Mater.*, 2011, **23**, 4428-4434.
44. Z. Ning, Z. Chen, Q. Zhang, Y. Yan, S. Qian, Y. Cao and H. Tian, *Adv. Funct. Mater.*, 2007, **17**, 3799-3807.

RSC Advances Accepted Manuscript

Graphical Abstract

View Article Online
DOI: 10.1039/C6RA11269B

Synthesis, two-photon absorption and aggregation-induced emission properties of multi-branched triphenylamine derivatives based on diketopyrrolopyrrole for bioimaging

Ji Yang, Haoqi Tan, Dongyu Li, Tao Jiang, Yuting Gao, Bo Li, Xue Qu, and Jianli Hua**

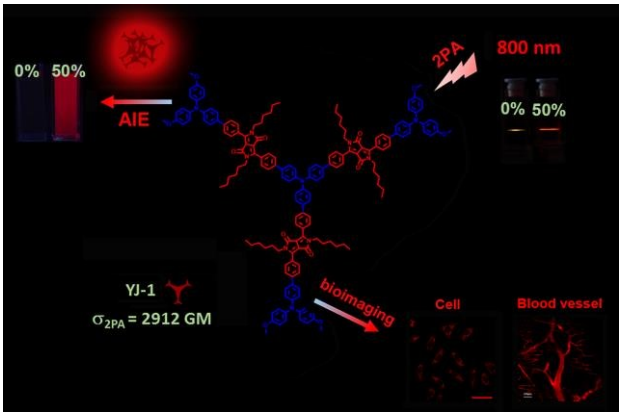

Three new diketopyrrolopyrrole (DPP)-based multi-branched derivatives **(YJ-1-3)** with AIE and 2PA properties were designed and synthesized. **YJ-1** containing triphenylamine donor was applied for cell imaging and two-photon excited fluorescence in vivo imaging of mouse ear.

Published on 10 June 2016. Downloaded by California State University at Fresno on 12/06/2016 07:52:02.

RSC Advances Accepted Manuscript